

ESR Studies on Mn(II) Ions in Japanese Marine Pearls

Yong LI, Kunihiko TAJIMA, Kazuhiko ISHIZU,* Nagao AZUMA,† and Kiyonori MIYOSHI††

Department of Chemistry, Faculty of Science, Ehime University, Matsuyama 790

†Faculty of General Education, Ehime University, Matsuyama 790

††Department of Metallurgical Engineering, Niihama National College of Technology, Niihama 792

(Received March 14, 1988)

X-band and Q-band ESR measurements of Mn(II) ions contained in Japanese cultured marine pearls and pearl oyster (*Pinctada fucata*) were carried out at room temperature. The ESR spectra observed for the powdered samples of nacreous and prismatic layers revealed the ESR hyperfine structures typical to Mn(II) in an aragonite lattice and a calcite lattice, respectively. The ESR spectra were interpreted with the following spin Hamiltonian.

$$\mathcal{H} = g\beta H \cdot S + aS \cdot I - g_n\beta_n H \cdot I + D[S_z^2 - S(S+1)/3] + E(S_x^2 - S_y^2)$$

The resonance fields for all the $M = +1/2 \leftrightarrow M = -1/2$ ESR transitions were derived, with the third-order corrections all taken into account. The zero-field splitting parameters D and E for Mn(II) ions in these biominerals were estimated by computer simulations of the ESR line shapes. The estimated parameters for the nacreous Mn(II) ion ($D=20.8$ mT, $E=6.9$ mT) are apparently different from those for the prismatic Mn(II) ion ($D=8.5$ mT, $E=1.4$ mT).

First observation of the ESR of marine seed pearls was recently reported by Ishizu et al.¹⁾ They found that pearls containing the blackish materials gave a more intense ESR signal of an organic free radical assignable to that of melanin, as justified from the isotropic g -factor, line width, and microwave saturation behavior. It has also been reported that the blackish pearls revealed ESR spectra resemblant to those of the Mn(II) ion in the calcite lattice, whereas the ESR spectra of the Mn(II) ion in satin white and pale yellow pearls resemble those of Mn(II) ion in the aragonite lattice. Accordingly one will expect that a detailed analysis of the Mn(II) ESR spectrum will provide useful information to characterize the crystal structure of the calcification phase in terms of the ESR crystal field parameters. In this paper, the ESR spectra of the Mn(II) ion contained in typical Japanese marine pearls have been analyzed and their detailed parameters have been discussed. Those of pearl oyster (*Pinctada fucata*) have also been examined, as typical ESR spectra of the Mn(II) ion in the calcite lattice.

The crystal field characters of the Mn(II) ion are discussed based on a spin Hamiltonian involving an isotropic g -factor, isotropic hyperfine structure term a , and zero-field splitting parameters D and E , where the third-order perturbation corrections were all calculated. The D and E values have been obtained by computer simulation of the observed ESR line shapes.

Experimental

The pearls and pearl oyster (*Pinctada fucata*) were respectively cultured and collected at Uwa Sea, Ehime Prefecture, Japan. The pearls were pulverized after removal of their artificial nuclei. The shells were washed to remove the sludge and scales of acorn barnacles that covered them, then the powdered sample was collected from the outer surface, i.e. the prismatic layer, of the shell. Satin white and blackish pearls were used as typical reference materials.

X-band and Q-band ESR spectra were respectively recorded by a JEOL-FE-2XG X-band spectrometer and by a JEOL-ES-SQ4 Q-band spectrometer operating with 100 kHz magnetic-field modulation. Li-TCNQ ($g=2.0025$) and Cr(III) in MgO ($g=1.9800$) were used as standard g markers. The magnetic fields were calibrated with the hyperfine splitting of Mn(II) in MgO (8.69 mT).

The computer program used for simulation of the observed ESR spectra of the powdered samples is similar to those of Pilbrow et al. and Belford et al.²⁾ The calculations were carried out on a FACOM M-180II AD computer at the Data Processing Center of this University.

Results and Discussion

The spin Hamiltonian appropriate for Mn(II) ion ($S=5/2$, $I=5/2$) can be written by

$$\mathcal{H} = g\beta H \cdot S + aS \cdot I - g_n\beta_n H \cdot I + D[S_z^2 - S(S+1)/3] + E(S_x^2 - S_y^2) \quad (1)$$

where all symbols have their usual meaning, and we assume that g and a are both isotropic, which is a good approximation for an S state ion.

Approximate solutions of the spin Hamiltonian have been reported by various authors. In the ESR spectra of Mn(II) ions, forbidden transitions ($\Delta M = \pm 1$, $\Delta m = \pm 1$) have been usually observed in addition to the allowed transitions ($\Delta M = \pm 1$, $\Delta m = 0$). Bleaney et al.³⁾ previously explained the positions of the forbidden lines and their remarkably large intensity relative to the allowed transition, with application of the perturbation procedure, where they have restricted their third-order corrections to the terms of aD^2 . Later, although the theoretical calculations have been reviewed by several authors. Their results were obtained by assuming some third-order corrections to be zero but these were not suitable for the simulation of the present spectra.⁴⁾ Therefore, we have derived the general solution which includes all the third-order corrections.

Theoretically, the spectrum of Mn(II) ion with D , $a \ll g\beta H_0$ exhibits fine structure due to five transitions with transition probability ratio of 5:8:9:8:5, each of which splits into six hyperfine lines and five pairs of forbidden hyperfine lines. However, we have not observed any clear fine structure due to the transition other than the strongest central fine structure transition ($M=1/2 \leftrightarrow M=-1/2$). One of the reasons for this may be that the concentrations of Mn(II) ions in the samples were too low to observe all the transitions. In fact, the contents of manganese ions in marine pearls and shells are one order less than those in fresh water ones.⁵⁾

When the angle between the magnetic field direction and the z axis, and the angle between the projection of the magnetic field direction on the x - y plane and the x axis (θ and φ) are employed, the resonance fields concerned with the central fine structure transition are given for the allowed transitions [$(+1/2, m) \leftrightarrow (-1/2, m)$] by,

$$H = H_0 - am/g\beta + [8(16\nu - 2w) + a^2(4m^2 - 35)]/8g^2\beta^2H_0 - am[a^2(4m^2 - 65) + 16(72\nu - w + 2au)]/8g^3\beta^3H_0^2 \quad (2)$$

for the forbidden transitions [$(+1/2, m-1) \leftrightarrow (-1/2, m)$],

$$H = H_0 - a(2m+1)/2g\beta - g_n\beta_n H_0/g\beta + [8(16\nu - 2w) + a^2(4m^2 + 4m - 67)]/8g^2\beta^2H_0 - a(2m+1)[a^2(4m^2 + 4m - 195) + 16(72\nu - w + 4au)]/16g^3\beta^3H_0^2 \quad (3)$$

and for the forbidden transitions [$(+1/2, m) \leftrightarrow (-1/2, m-1)$],

$$H = H_0 - a(2m+1)/2g\beta + g_n\beta_n H_0/g\beta + [8(16\nu - 2w) + a^2(2m+1)^2]/8g^2\beta^2H_0 - a(2m+1)[a^2(4m^2 + 4m + 73) + 16(72\nu - w)]/16g^3\beta^3H_0^2 \quad (4)$$

where

$$H_0 = h\nu/g\beta \quad (5)$$

$$u = D(3\cos^2\theta - 1) + 3E\sin^2\theta\cos 2\varphi \quad (6)$$

$$v = (D - E\cos 2\varphi)^2\sin^2\theta\cos^2\theta + E^2\sin^2\theta\sin^2 2\varphi \quad (7)$$

$$w = [D\sin^2\theta + E\cos 2\varphi(\cos^2\theta + 1)]^2 + 4E^2\cos^2\theta\sin^2 2\varphi \quad (8)$$

The transition probabilities of the above forbidden transitions relative to the allowed transitions are given by

$$I = 64\nu[35 - 4m(m+1)]/g^2\beta^2H_0^2 \quad (9)$$

It has been well documented that the prismatic layer, or the outer surface, of the shell has the form of calcite. The calcite lattice has a symmetry octahedral unit. This reflects to the typical ESR spectrum with relatively high axial symmetry of the zero-field splitting as shown in Fig. 1(a). The six main lines arise from the allowed transitions, and five weak pairs of lines between the main lines are ascribed to the forbidden transitions. This spectrum is the same as that of the shell (*Balanus balanoides*) but some difference can be

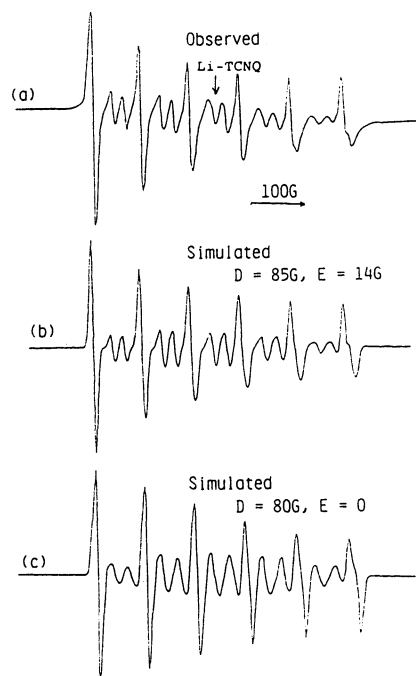


Fig. 1. (a): The X-band ESR spectrum observed at room temperature for Mn(II) ion in the prismatic layer of shell (*Pinctada fucata*). (b) and (c): The computer simulated ESR spectra for (a).

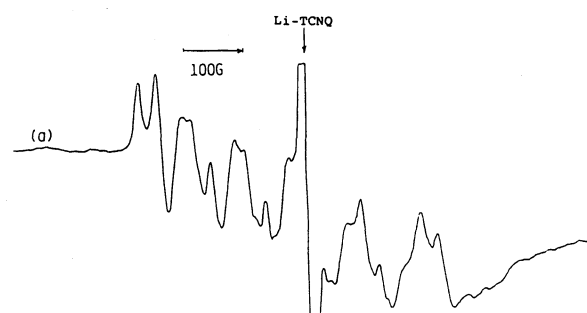


Fig. 2. The X-band ESR spectrum observed at room temperature for Mn(II) ion in the nacreous layer of the cultured marine pearl.

seen in the line width of the shell (*Mytilus edulis*), both reported by Chasteen et al.^{6,7)} In the case of the marine shell (*Mytilus edulis*) reported so far, the ESR line width is sharp because of the longer spin-lattice relaxation. The zero-field splitting parameters can therefore be determined from the observed spectrum. However, in the present case, those parameters have been estimated by computer simulation of the ESR line shape, since the fine structures are poorly observed. The apparent ESR intensities for the allowed transitions are decreased on the higher magnetic field side, as the D value is increased. For convenience, the E value is usually taken to be zero in the calcite case. However, the line shape of the spectrum simulated by taking account of the E term is similar to the observed one, Fig. 1(b), in comparison with that which is simulated by omitting the E term, Fig. 1(c).

In contrast to the ESR spectrum of the prismatic layer, the X-band ESR spectrum of the nacreous layer of the cultured pearls appears to be very complicated, as shown in Fig. 2. The nacreous layer is composed of calcium carbonate in the form of aragonite. Because a metal ion in the aragonite lattice takes an unusual lower symmetrical nine-coordinate geometry,⁸⁾ the Mn(II) ion possesses the large zero-field interaction which brings the strong forbidden transition on the observed ESR spectrum. Consequently, the allowed and forbidden transition absorptions are overlapped each other; thus the Mn(II) ESR spectra become complicated with high anisotropy. According to Eq. 9, the forbidden transition intensity will be effectively reduced and the ESR hyperfine structure much simplified when the magnetic field increases. Actually, the Q-band ESR spectrum observed for the powdered sample of the nacreous layer is less complex and an effective reduction in the forbidden transition absorptions can be observed, Fig. 3(a). A similar Q-band ESR spectrum was reported for clam shell (*Mya arenaria*) by Chasteen et al.,⁹⁾ where the zero-field splitting parameters were determined from the hyperfine lines due to the second- and third-order terms in the perturbation equations. The spectrum for the pearl is less resolved than that for the clam shell. Therefore, the computer

simulation of the Q-band ESR line shape has also been carried out to estimate the D and E values, as summarized in Table 1.

In the case of calcite, the present D value is similar to that reported by Chasteen et al.,⁹⁾ although the method used to determine the zero-field splitting parameters are different. The contribution of the E value was found to be larger than what we had expected from the usual approximation of setting the same term to zero. Thus the importance of the E term is demonstrated for the metal ion doped in a calcite lattice. The estimated D and E values for the Mn(II) ion in the aragonite phase of the marine pearl are different from those reported for the same phase in clam shell (*Mya arenaria*) by Chasteen et al.⁹⁾ The present D and E values for the marine pearl are respectively less and larger than the values for their shell, as shown in Table 1.

The range of ratio $r(=E/D)$ is distributed from 0 to $1/3$, and it is taken to be a parameter which indicates a degree of ligand field symmetry. When the r value is zero, the ligand field has perfect axial symmetry, and if the r value is $1/3$, that means perfect rhombic symmetry. It is interesting that the r value of the Mn(II) ion determined for the marine pearl is about $1/3$. This means that the nacreous layer of the marine pearl is composed of aragonite which is highly distorted by the metal coordination geometry.

As described earlier, the satin white and the pale yellow pearls revealed ESR hyperfine structure ascribed to the Mn(II) ion contained in the aragonite matrix of the nacreous layer. The pearls containing blackish materials usually gave a mixed hyperfine splitting of prismatic Mn(II) and that of Mn(II) ascribed to the species in the aragonite matrix. In this case, the detailed analysis of the line shape is difficult, because the line shape analysis of the X-band ESR of Mn(II) in the aragonite lattice is much more complicated due to the overlapping of the multi-forbidden transition. The further calculation of the line shape in this case is now under way.

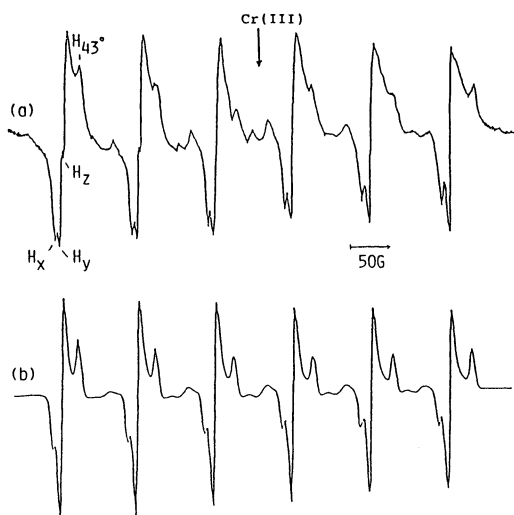


Fig. 3. (a): The Q-band ESR spectrum observed at room temperature for Mn(II) ion in the nacreous layer of the cultured marine pearl. (b): The computer simulated ESR spectrum for (a).

Table 1. ESR Parameters for Mn(II) Ions in the Calcite Lattice in the Prismatic Layer of Marine Shell (*Pinctada fucata*) and in the Aragonite Matrix in Nacreous Layer of the Marine Pearl

	g	a/mT	D/mT	E/mT	E/D	
Calcite	2.006	9.40	8.50	1.40	0.16	This work
	2.001	9.38	8.63	—	—	Ref. 7
Aragonite	2.004	9.60	20.80	6.90	0.33	This work
	2.006	9.40	25.00	4.20	0.17	Ref. 9

The authors wish to express their sincere thanks to Mr. Terumi Kobata who provided the valuable samples of pearls and shells, we also gratefully acknowledge Professors Noboru Hirota and Hiroaki Ohya-Nishiguchi of Kyoto University for their measurement of Q-band ESR spectra. This work was partially supported by the Grant-in-Aid for Scientific Research (No. 63540491) from the Ministry of Education, Science and Culture. The X-band ESR measurements were carried out at the Advanced Instrumentation Center for Chemical Analysis of this University.

References

- 1) K. Ishizu, *SHINJU*, No. 189, 4 (1985); K. Ishizu, R. Ikeda, K. Tajima, and K. Miyoshi, *Nippon Kagaku Kaishi*, 1986, 93.
- 2) A. D. Toy, S. H. H. Chaston, J. R. Pilbrow, and T. D.

Smith, *Inorg. Chem.*, **10**, 2219 (1971); J. R. Pilbrow and M. E. Winfield, *Mol. Phys.*, **25**, 1073 (1973); L. K. White and R. L. Belford, *J. Am. Chem. Soc.*, **98**, 4428 (1976).

3) B. Bleaney and R. S. Rubins, *Proc. Phys. Soc. (London)*, **77**, 103 (1961); corrigendum, *ibid.*, **78**, 778 (1961).

4) L. M. Matarresse, *J. Chem. Phys.*, **34**, 336 (1962); V. J. Folen, *Phys. Rev.*, **125**, 1581 (1962); B. C. Cavenett, *Proc. Phys. Soc. (London)*, **84**, 1 (1964); H. W. de Wijn and R. F. van Balderen, *J. Chem. Phys.*, **46**, 1381 (1967).

5) K. Wada, *Housekigaku Kaishi*, **2**, 3 (1975); **8**, 151 (1981).

6) S. C. Blanchard and N. D. Chasteen, *Anal. Chim. Acta*, **82**, 113 (1976).

7) S. C. Blanchard and N. D. Chasteen, *J. Phys. Chem.*, **80**, 1362 (1976).

8) J. P. R. De Villiers, *Am. Mineral.*, **56**, 758 (1971).

9) L. K. White, A. Szabo, P. Carkner, and N. D. Chasteen, *J. Phys. Chem.*, **81**, 1420 (1977).
